Supplement to: Signalling centre vortices coordinate collective behaviour in social amoebae

Hugh Z Ford, Angelika Manhart & Jonathan R Chubb

1 Mathematical Model

In this section we give a detailed description of the computation model used to mimic and examine the collective dynamics of *Dictystelium* cells.

1.1 General Model Set-up

We use a hybrid computational model in two space dimensions. Cells are modelled as discrete elements, while the external cAMP concentration ([cAMP]) is represented as a continuous function. Cells are labelled by index $i = 1, \dots, N$, where N is the total number of cells. Each cell has a number of properties (position, speed, internal signalling dynamics, etc.). Cells produce external cAMP, which diffuses and decays. Cells also sense external cAMP, which influences their internal dynamics and movement. The spatial domain is $\Omega = [-L/2, L/2]^2 \subset \mathbb{R}^2$, where $L > 0$ is the domain size. The external [cAMP] at position x and time t is denoted by $c(x,t)$ for $t \geq 0$ and $x \in \Omega$ and cells are positioned at $X_i(t) \in \Omega$.

1.2 Internal Signalling Dynamics

Several models of internal cAMP dynamics have been suggested [2, 9, 7, 6, 5]. We choose to work with the model used in [9], which has been shown to be able to reproduce a wider range of experimental observations than other models [4]. The model is based on the famous FitzHugh-Nagumo model [1, 8], originally developed for spike generation in axons.

Let $A_i(t)$ and $I_i(t)$ represent activator and inhibitor dynamics of the i-th cell. Note that while they do not represent concentrations of specific molecules, we assume that the value of the activator determines cAMP release to the exterior of the cell. The dynamics are governed by

$$\begin{aligned} \tau \dot{A}_i &= A_i - \frac{1}{3}A_i^3 - I_i + \alpha \log\left(1 + \frac{c_i}{\kappa}\right), \\ \tau \dot{I}_i &= \varepsilon \left(A_i - \gamma I_i + \mu\right), \end{aligned} \tag{1}$$

where $c_i = c(X_i(t), t)$ is the concentration of external cAMP experienced by the i-th cell. We use the parameters from [9] and fit the time scale parameter τ to match the experimentally measured spiking frequency (see Tab. 1).

1.3 External cAMP dynamics

External cAMP is secreted by active cells. We define active cells as having a positive activator value $A_i > 0$ [9]. Once secreted, we assume external cAMP diffuses and decays. We note that other, more complicated dynamics of external cAMP have been used (e.g. active degradation by cells, [3]), however here we chose to omit such potential effects in the interest of simplicity. We use

the following equation

$$\partial_t c = D\,\partial_x^2 c - g\,c + a\sum_{i=1}^{N} H(A_i)\,\delta_d(x - X_i), \tag{2}$$

where D is the diffusion constant, g the decay rate and a the external cAMP secretion rate of active cells. H is the Heaviside function, i.e. only for $A_i > 0$ cells secrete cAMP, and δ_d denotes a smooth approximation of the Dirac delta. For numerical efficiency we use the product of two one-dimensional bump functions, i.e. if $x = (x_1, x_2)$, then $\delta_d(x) = b_d(x_1)b_d(x_2)$, where $b_d(r) = \frac{1}{Z}e^{-\frac{1}{1-(r/d)^2}}$ for $r < d$ and zero otherwise. The constant Z is a normalisation constant chosen such that δ_d has mass 1. The parameter d has units of space and can be interpreted as the size over which an activated cell secretes cAMP. Since we don't measure external cAMP explicitly, we don't specify the units of external cAMP, but just refer to the units as "conc". For parameters see Table 1.

1.4 Chemotaxis model

Numerical and experimental results indicate that while the gradient of external cAMP plays a critical role in determining cell direction, whether cells are sensitive to the gradient and how this in turn affects their velocity remains largely unclear.

Data-driven identification of chemotaxis model. A data-driven approach was used to infer an accurate yet simple mathematical model of single-cell *Dictyostelium* chemotaxis in response to dynamics external [cAMP] fields. To achieve this, we first used equation (2) to predict the external [cAMP] field using the experimentally measured cell positions and internal cAMP states as inputs. Using the inferred [cAMP] field we generated the time series (2 hours, 5 second intervals) for the external [cAMP] magnitude and gradient for each cell (in addition to the cell signalling state and velocity) in the central 1mm x 1mm area of the experimental field of view (1.2mm x 1.2mm). We then systematically compared how well the predicted external [cAMP] field can explain measured cell movement under various chemotaxis model assumptions. We started with simple models such as:

$$\dot{\boldsymbol{X}}_i = \alpha\,\nabla c_i\ , \tag{3}$$

which assumes that moves constant move towards higher [cAMP]. Here $\dot{\boldsymbol{X}}_i$ is the cell velocity and $|\nabla c_i|$. The Matlab function fminsearch was used to identify parameter values that minimise the mean difference in the measured and predicted direction and magnitude of cell velocity for each cell track. We then identified the shortcoming of each model, and added model complexity. For example, from equation 3, we incorporated receptor desensitisation, yielding the same model as in Ref. [3]:

$$\dot{\boldsymbol{X}}_i = \alpha\,s_i\,\nabla c_i \tag{4}$$

$$\dot{s}_i = a(1 - s_i) - b\,c_i\,s_i\ , \tag{5}$$

and s_i is the number of receptors on the surface and encapsulates receptor desensitisation. This process motivated the use of the chemotaxis model described in the next paragraph.

Best-fit chemotaxis model. We denote by $\theta_i(t) \in [0, 2\pi]$ and $v_i(t) \in \mathbb{R}$ the movement direction and speed of the i-th cell at time t respectively. Further we define a sensitivity for each cell, $s_i \in [0, 1]$, similar to what was used in [3]. We then use the identified model

$$\begin{aligned}
\dot{\theta}_i &= \alpha_m s_i |\nabla c_i| \sin(\theta_i^c - \theta_i), \\
\dot{v}_i &= \beta_m s_i |\nabla c_i| - \gamma_m v_i, \\
\dot{s}_i &= \sigma_m(1 - s_i) - \lambda_m c_i s_i,
\end{aligned} \tag{6}$$

where θ_i^c is the direction of the local gradient of external cAMP, evaluated at X_i and ∇c_i is the spatial gradient of external cAMP evaluated at $x = X_i$. The parameters α_m, β_m, γ_m, σ_m, λ_m are determined during the model identification and fitting method described above (see Tab. 1. The first equation models the turning of the cell towards the local gradient of external cAMP. The turning speed depends on a cell's sensitivity and the size of the cAMP gradient. The second equation describes adaptation of the cell speed. It drives cell speed to be proportional to $s_i|\nabla c_i|$, i.e. higher sensitivity and larger local gradients will lead to faster speeds. Finally, the third equation models sensitivity: If a cell experiences a high concentration of external cAMP c_i, it will become de-sensitised and it takes some time to become sensitive again. Note that if s_i is initially chosen in $[0, 1]$, the equation preserves this property.

For the final cell movement model we also model size exclusion effects between cells, by including a cell-cell repulsion term. This means θ_i and v_i are understood to mean the orientation and speed a cell would have if not in contact with other cells. We define as $d_{ij} = |X_i - X_j|$ the distance between the cell centres of the i-th and j-th cell. A cell's movement now follows

$$\dot{X}_i = v_i \left(\cos\theta_i, \sin\theta_i\right) + \rho_R \sum_{j\neq i, d_{ij}<d_R} \left(1 - \frac{d_{ij}}{d_R}\right) \frac{X_i - X_j}{d_{ij}}, \tag{7}$$

i.e. cells move with speed v_i in direction θ_i in the absence of cell-cell repulsion. The second term describes a cell-cell repulsion with maximal repulsion magnitude ρ_R, where only cells within a distance of d_R of each other exert a pushing force.

1.5 Initial and boundary conditions

We use no-flux boundary conditions for the external cAMP concentration, i.e. cAMP cannot leave the domain. Similarly cells cannot leave the domain. Since the dynamics cause a concentration of cells towards the spiral center, cells are being depleted from the very edge of the simulation domain and hence we only considered the middle part of the simulation domain to represent the biological situation.

For all numerical experiments we initialise cell positions X_i and orientations θ_i using a uniform random distribution on Ω and $[0, 2\pi]$ respectively. Cell sensitivities s_i were initially set to 1 and cell speeds v_i to 0. The initial external cAMP concentration, activator and inhibitor values were initialised as shown in Fig. 1. The values shown in Fig. 1 were created by disabling cell movement and 1. Letting a vertical cAMP wave moving from left to right across a periodic domain until it is equilibrated, 2. Setting the external cAMP in the upper-half of the domain to zero and setting the inhibitor value in the upper half on the domain to a high value (we used 2.5) and 3. Setting the boundary conditions to no-flux and restarting the simulation. This creates the spiral shown in Fig. 1.

1.6 Numerics

We solve (1), (2), (6), (7) numerically using Matlab.

External cAMP. We discretise $c(x, t)$ on a regular rectangular spatial grid using 50 gridpoints per mm length. To solve (2) we use a finite difference, implicit Euler method in time (time step Δt), using a central difference in space (spatial step Δx) discretisation for the diffusion term. The source term is taken explicitly, i.e. evaluated at the current time step.

Cell movement. The internal cAMP dynamics (1) as well as dynamics of the chemotaxis related quantities (6) are solved on $[t, t+\Delta t]$ using an the in-built Matlab solve ode45. Finally (7) is solved using an explicit Euler method (time step Δt).

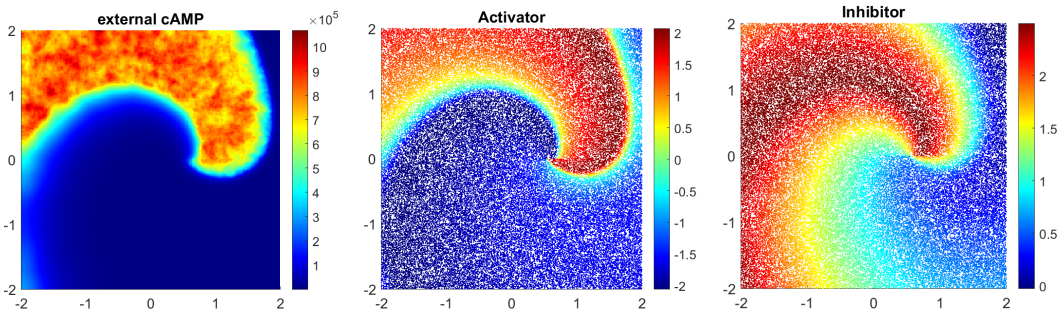

Figure 1: Initial conditions used. Spatial units are in mm, colorbar represent external cAMP concentration (left) and activator and inhibitor values (middle and right).

parameter/variable	meaning	value/unit	reference
$c(x,t)$	external cAMP concentration	conc	
$X_i(t)$	cell position	in (mm,mm)	
$A_i(t)$	cAMP activator	a.u.	
$I_i(t)$	cAMP inhibitor	a.u.	
$\theta_i(t)$	cell orientation	in radians	
$v_i(t)$	cell speed	in mm/min	
$s_i(t)$	cell sensitivity	in $[0,1]$	
τ	time scale of cAMP dynamics	0.167min	fitted
ε	activator and inhibitors time scales ratio	0.1	[9]
γ	inhibitor decay rate	0.5	[9]
μ	basal inhibitor production	1.2	[9]
α	cAMP response magnitude	0.058	[9]
κ	cAMP response threshold	10^{-5}conc	[9]
D	ext. cAMP diffusion constant	2.4×10^{-2}mm^2/min	[10]
g	ext. cAMP degradation rate	5/min	[10]
a	ext. cAMP secretion rate	10^3conc mm^2/min	[10]
d	ext. cAMP secretion length scale	0.1mm	estimated
α_m	maximal turning rate	3×10^{-6}mm/(min conc)	fitted
β_m	speed model parameter	10^{-8}mm^2/(min^{2}conc)	fitted
γ_m	speed model parameter	0.6/min	fitted
σ_m	re-sensitisation	150/min	fitted
λ_m	de-sensitisation	4×10^{-3}/(min conc)	fitted
ρ_R	maximal repulsion strength	0.1mm/min	guessed
d_R	cell radius	5×10^{-3}mm	measured
L	domain length	4mm	experiments
Δx	spatial step	0.02mm	
Δt	temporal step	0.05min	

Table 1: Parameters.

References

[1] Richard FitzHugh. Impulses and physiological states in theoretical models of nerve membrane. *Biophysical journal*, 1(6):445–466, 1961.

[2] Thomas Gregor, Koichi Fujimoto, Noritaka Masaki, and Satoshi Sawai. The onset of collective behavior in social amoebae. *Science*, 328(5981):1021–1025, 2010.

[3] Thomas Höfer, Jonathan A Sherratt, and Philip Kumar Maini. Dictyostelium discoideum: cellular self-organization in an excitable biological medium. *Proceedings of the Royal Society of London. Series B: Biological Sciences*, 259(1356):249–257, 1995.

[4] Chuqiao Huyan, Alexander Golden, Xinwen Zhu, Pankaj Mehta, and Allyson E Sgro. Robust coordination of collective oscillatory signaling requires single-cell excitability and fold-change detection. *bioRxiv*, 2021.

[5] Keita Kamino, Yohei Kondo, Akihiko Nakajima, Mai Honda-Kitahara, Kunihiko Kaneko, and Satoshi Sawai. Fold-change detection and scale invariance of cell–cell signaling in social amoeba. *Proceedings of the National Academy of Sciences*, 114(21):E4149–E4157, 2017.

[6] Mineko Maeda, Sijie Lu, Gad Shaulsky, Yuji Miyazaki, Hidekazu Kuwayama, Yoshimasa Tanaka, Adam Kuspa, and William F Loomis. Periodic signaling controlled by an oscillatory circuit that includes protein kinases erk2 and pka. *Science*, 304(5672):875–878, 2004.

[7] Jean-Louis Martiel and Albert Goldbeter. A model based on receptor desensitization for cyclic amp signaling in dictyostelium cells. *Biophysical journal*, 52(5):807–828, 1987.

[8] Jinichi Nagumo, Suguru Arimoto, and Shuji Yoshizawa. An active pulse transmission line simulating nerve axon. *Proceedings of the IRE*, 50(10):2061–2070, 1962.

[9] Allyson E Sgro, David J Schwab, Javad Noorbakhsh, Troy Mestler, Pankaj Mehta, and Thomas Gregor. From intracellular signaling to population oscillations: bridging size-and time-scales in collective behavior. *Molecular systems biology*, 11(1):779, 2015.

[10] Estefania Vidal-Henriquez and Azam Gholami. Spontaneous center formation in dictyostelium discoideum. *Scientific reports*, 9(1):1–11, 2019.